


# SCIENTIFIC REPORTS



OPEN

## Dynamic interaction between basin redox and the biogeochemical nitrogen cycle in an unconventional Proterozoic petroleum system

Grant M. Cox<sup>1</sup>, Pierre Sansjofre<sup>2</sup>, Morgan L. Blades<sup>1</sup>, Juraj Farkas<sup>1</sup> & Alan S. Collins<sup>1</sup> 

Precambrian hydrocarbons and their corresponding source rocks are distinctly different from their Phanerozoic counterparts, having been deposited in persistently anoxic environments in ecosystems dominated by bacteria. Here, we show that cyclic enrichment of organic matter in the world's oldest hydrocarbon play (ca. 1.38 Ga), is not associated with flooding surfaces and is unrelated to variations in mineralogy or changes in the relative rate of clastic to biogenic sedimentation—factors typically attributed to organic enrichment in Phanerozoic shales. Instead, the cyclic covariation of total organic carbon,  $\delta^{15}\text{N}$ ,  $\delta^{13}\text{C}$  and molybdenum are explained by the feedback between high levels of primary productivity, basin redox and the biogeochemical nitrogen cycle. These factors are important in constraining productivity in the marine biosphere, the development of Precambrian hydrocarbon source rocks, and more generally in understanding oxygenation of the ocean and atmosphere through Earth history; as all are ultimately related to organic carbon burial.

High total organic carbon (TOC) content within sediments has been attributed to various factors, including high primary productivity<sup>1</sup>, high nutrient fluxes due to warm and wet climatic conditions<sup>2,3</sup>, basin redox conditions facilitating the preservation of organic matter<sup>4</sup>, mineralogical controls on organic carbon export<sup>5–7</sup> and changes in the relative rate of clastic to biogenic sedimentation<sup>8</sup>. Understanding these processes, which likely vary in both space and time, are important in constraining the development of hydrocarbon source rocks and more generally in understanding oxygenation of the ocean and atmosphere through Earth history; as both are tied to organic carbon burial.

Primary productivity is generally accepted to be limited by the availability of phosphorus, dissolved inorganic nitrogen (DIN:  $\text{NH}_4^+$ ,  $\text{NO}_3^-$ ) and bio-essential trace metals<sup>9–12</sup>. Furthermore, it is widely appreciated that high levels of primary productivity and organic matter export can influence basin redox. In particular, Johnston *et al.*<sup>13</sup> demonstrated the relationship between high levels of organic carbon export and euxinia, while Anbar and Knoll<sup>11</sup> highlighted how basin redox, in particular euxinia, influences nutrient concentrations, in particular trace nutrients such as molybdenum, with flow on effects for bioavailable nitrogen. Furthermore, recent work has shown that the magnitude of organic matter supply also affects the rate of denitrification<sup>14</sup> and consequently bioavailable nitrogen concentrations. Such effects on nitrogen availability naturally affect primary productivity and organic carbon burial, as biologically available nitrogen can limit photosynthesis and is often referred to as the proximal limiting nutrient<sup>10</sup>. Building upon these general observations, we present  $\delta^{15}\text{N}$  and  $\delta^{13}\text{C}$  data from the hydrocarbon-bearing Roper Group of the greater McArthur Basin of northern Australia. These suggest that the cyclic production of high TOC sediments in this Mesoproterozoic black shale succession is controlled by oscillations between nitrogen replete and nitrogen limited conditions. These are hypothesized to be a consequence of the coupling of elevated primary productivity, high degrees of organic carbon export, basin redox and the biogeochemical nitrogen cycle. These processes interact to impact nitrogen availability through changes in the balance between nitrogen supply via  $\text{N}_2$  fixation and nitrogen loss through denitrification.

<sup>1</sup>University of Adelaide, Adelaide, S.A., 5005, Australia. <sup>2</sup>UMR 6538, Laboratoire Géosciences Océan, Institut Universitaire Européen de la Mer, rue Dumont d'Urville, 29280, Plouzané, France. Correspondence and requests for materials should be addressed to G.M.C. (email: [grantmcox@me.com](mailto:grantmcox@me.com))

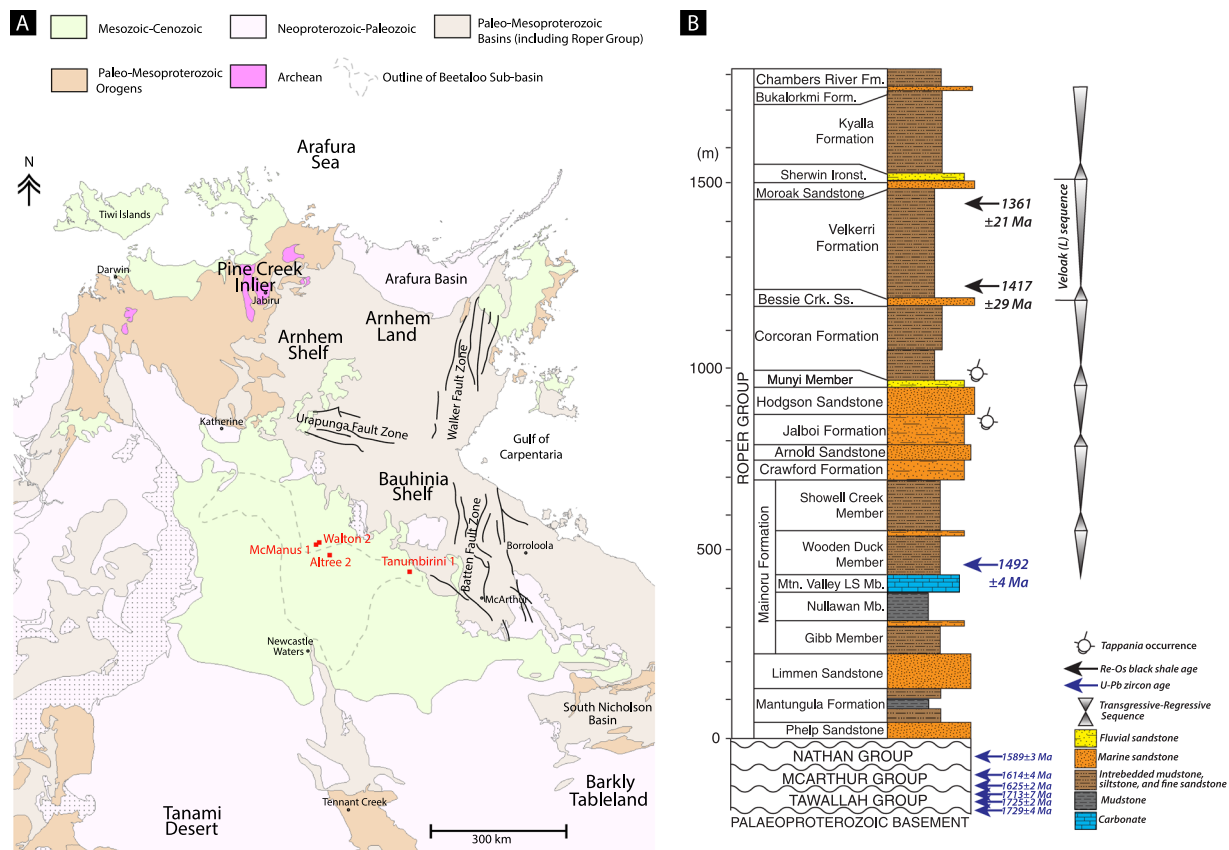


**Figure 1.** Regional geology and stratigraphic sequence. (A) Distribution of sedimentary basins of northern Australia. (B) Stratigraphic column for the Roper Group showing major transgressive-regressive sequences. Reproduced from ref.<sup>36</sup>.

## Nitrogen Isotopes

In models for stratified oceans with only a shallow oxic layer<sup>15,16</sup>, a condition widely considered to characterise the Proterozoic<sup>17</sup>, the availability of bioavailable nitrogen would be tied to prokaryotes (i.e. cyanobacteria) that perform  $N_2$ -fixation (i.e. diazotrophy), along with remineralised nitrogen. The loss of bioavailable nitrogen is achieved either through heterotrophic denitrification and/or anaerobic ammonium oxidation (i.e. ANAMMOX). It is widely held that diazotrophs are at a competitive disadvantage under nitrogen replete conditions. Consequently, it is only under nitrogen-limited conditions that diazotrophs are expected to fix appreciable amounts of nitrogen. As the diazotroph biomass has an average  $\delta^{15}N$  of  $\sim -1\%$ , and can range from  $-3\%$  to  $+1\%$ <sup>18</sup>, any increase in  $N_2$ -fixation in response to nitrogen limitation tends to decrease the  $\delta^{15}N$  of DIN toward pure  $N_2$ -fixation values (i.e.  $-3\%$  to  $+1\%$ ). In contrast to  $N_2$  fixation, denitrification and anaerobic ammonium oxidation preferentially return light nitrogen to the atmosphere, leaving the residual pool of bioavailable nitrogen isotopically heavier<sup>19,20</sup>. Nitrification and biological assimilation produce large fractionations in nitrogen isotopes<sup>21,22</sup>, however, these fractionations are ordinarily not expressed, as such processes are nearly quantitative. This is observed in the modern marine system through the 1:1 correspondence between  $\delta^{15}N_{\text{sedimentary}}$  and  $\delta^{15}N_{\text{nitrate}}$  (e.g. Fig. 34.6 – ref.<sup>23</sup>). Therefore, nitrogen isotopes typically trace the balance between  $N_2$ -fixation and heterotrophic denitrification and anaerobic ammonium oxidation, with the latter two being highly redox dependent being carried out under sub-oxic conditions<sup>24–26</sup>.

## Geology

The Roper Group of northern Australia, is the younger of four unconformity-bound sedimentary packages of the much larger greater McArthur Basin<sup>27,28</sup>. Significant lateral thickness changes occur within the Roper Group. It is thin ( $\sim 1$ – $2$  km) in the vicinity of the east-west trending Urupunga Fault Zone, of moderate thickness over the Broadmere Inversion Structure ( $\sim 2$  km<sup>29</sup>), and thinnest ( $< 500$  m) over the north-south trending Batten Fault Zone (Fig. 1A)<sup>28,30–32</sup>. Southwest of the Batten Fault Zone, the Roper Group thickens to  $> 5$  km in the Beetaloo Sub-basin<sup>28,30–33</sup> (Fig. 1A), which is interpreted to represent the main depo-centre of the Roper Seaway<sup>30,32</sup>.

The Velkerri Formation, a black-shale dominated unit within the Roper Group, is a key environmental archive for the early-middle Mesoproterozoic due to its exceptional thickness, well-constrained age ( $1386 \pm 13$  Ma to  $1361 \pm 21$  Ma<sup>34,35</sup>), large variations in organic carbon content, and low metamorphic grade<sup>36,37</sup>. Prior work has shown that the Velkerri Formation hosts some of the oldest known 'live' hydrocarbon occurrences<sup>38</sup>, and continues to generate substantial interest as an unconventional gas play, with an estimated in place gas resource of 118 trillion cubic feet<sup>37</sup>. Recent production testing has resulted in the successful hydraulic fracturing of this

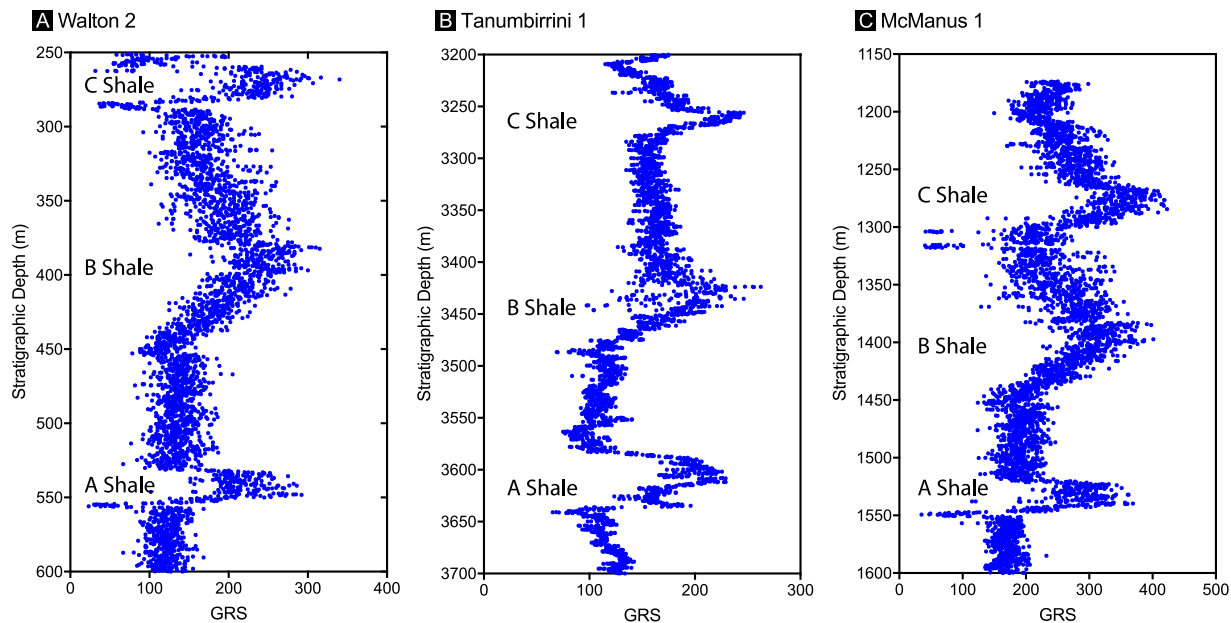


**Figure 2.** Gamma ray spectra (GRS) for regionally distributed sections of the Velkerri Formation. See Fig. 1 for well locations.

Mesoproterozoic formation resulting in substantial gas flows<sup>39</sup> making this one of the oldest proven unconventional hydrocarbon plays.

The Velkerri Formation is the initial deep water facies of the Veloak sequence<sup>30</sup> (Fig. 1B), which comprises the dominantly basinal facies of the Velkerri Formation transitioning up-section into cross-bedded sandstones of the Moroak Sandstone (Fig. 1B). The Velkerri Formation is formally divided into three distinct members, the Kalala (lower), Amungee (middle) and Wyworrie (upper) members<sup>40</sup>. The Amungee Member is the principal black shale facies with total organic carbon contents reaching ~10%<sup>36,37</sup>.

Detailed sedimentary petrology of the Amungee Member has shown that the facies was deposited below storm weather wave base and is composed of thinly laminated, grey-green to dark grey clays, pale grey silts and rare, fine-grained sands<sup>40,41</sup>. Organic enrichment within the Amungee Member occurs principally as three prominent horizons that are informally referred to as the A, B and C organofacies. Gamma Ray Spectra (GRS) reveals that these organofacies are a feature of the Amungee Member at the regional scale (Fig. 2). The organic-rich and organic-poor intervals show no systematic relationship to either grain size or mineralogy (Fig. 3). Based on this observation it was noted that the organic-rich and organic-poor intervals do not reflect changes in the energy of deposition or water depth, but must reflect changing water column biochemistry<sup>41</sup>.

## Methods

**Samples.** Samples were obtained from the petroleum well Atree-2 drilled by Pacific Oil and Gas and now housed in the Northern Territory Geological Surveys core facility in Darwin, N.T. The Velkerri Formation, which forms the basis of this study was intercepted at depths between 391.72 m and 1229.65 m. Rock samples were broken into ~2 cm<sup>3</sup> fragments and the resulting chips were milled in a tungsten carbide mill until the powder could pass through a 75 µm mesh resulting in a homogenous sample powder.

**Bulk rock pyrolysis.** Pyrolysis measurements were undertaken using a Weatherfords SRA. Crucibles were loaded into the carousel and heated under inert nitrogen in both the pyrolysis (to obtain S1, S2, T<sub>max</sub> and S3 peaks) and oxidation ovens (to obtain the S4 peak). The pyrolysis oven was first held at 300 °C for 5 minutes and ramped at 25 °C per minute from 300 °C to 650 °C. The oxidation oven was held at 400 °C for 3 minutes, ramped at 20 °C per minute from 400 °C to 850 °C and held at 850 °C for 5 minutes. The flame ionisation detector (FID) was calibrated by running IFP standard '160000' in 'standard' mode. The IR Analysers were calibrated against standard gas with known concentration of CO<sub>2</sub> and CO. An analysis blank was run as 'blank' mode with the sample batch and the blank data was automatically subtracted from all analyses. An internal standard was also run first with each batch to ensure the instrument status. The results were processed with Optkin 3.0 software where peak heights and geochemical indices including Total organic carbon (TOC), Oxygen Index (OI), Hydrogen Index (HI) and Production Index (PI) are automatically calculated.

**XRD analysis.** X-ray diffraction (XRD) analysis was undertaken on the raw powder utilising a Bruker D4 XRD. Quantification of the multiphase mixtures using Rietveld quantitative analysis was undertaken using the DIFFRAC<sup>™</sup> software suite.

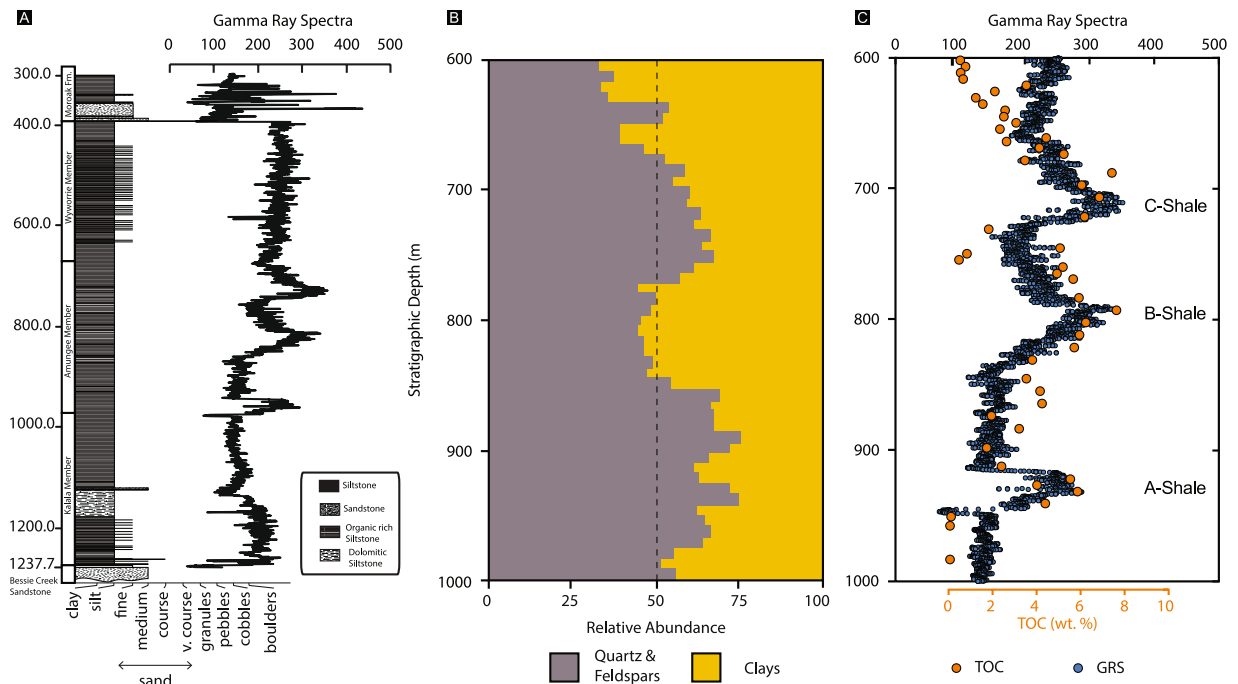


**Figure 3.** (A) Stratigraphic log of the Atree 2 well along with full gamma ray spectra. (B) Relative abundance of major mineral groupings based on high resolution XRD analysis of the Atree 2 well. (C) TOC overlain on expanded gamma ray spectra for Atree 2.

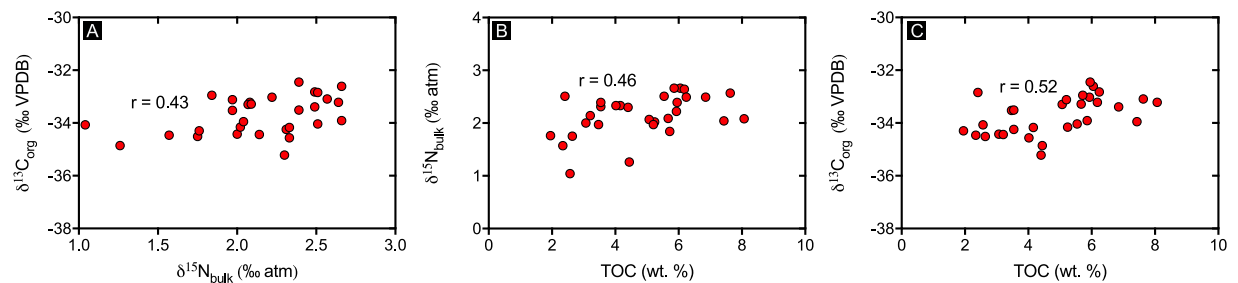


**Figure 4.** (A)  $\delta^{13}\text{C}_{\text{org}}$  vs.  $\delta^{15}\text{N}_{\text{bulk}}$ , (B)  $\delta^{15}\text{N}_{\text{bulk}}$  vs. TOC and (C)  $\delta^{13}\text{C}_{\text{org}}$  vs. TOC. R values are Spearman Correlation co-efficient and all are significant at  $\alpha = 0.05$ . Two tailed p values are 0.0182, 0.0112 and 0.0036 respectively.

**Carbon and nitrogen stable isotope analyses.** 1 to 2 grams of sample powder were treated with excess 3N HCl for 24 hours to remove trace carbonate minerals. Insoluble residual was centrifuged and rinsed with deionized water until supernatant achieved a pH of 4. Isotopic analyses for nitrogen and carbon were performed using a Euro EA Elemental Analyzer coupled to a Nu Horizons continuous-flow stable isotope mass spectrometer. Analyses were performed in the stable isotope laboratory at the University of Adelaide. Powdered, decarbonated samples were weighed and sealed in tin capsules for isotopic analysis and were combusted at 1050 °C. Data are reported using delta notation relative to atmospheric  $\text{N}_2$  for nitrogen and the Vienna Pee Dee Belemnite International Standard (V-PDB) for carbon.  $\delta^{15}\text{N}$  were calibrated to international reference standards IAEA N1, N2, NO-3, and USGS 25, 32, 40 and 41.  $\delta^{13}\text{C}$  was calibrated to IAEA CH-6 and CH-7; USGS 24, 40, and 41; and NBS-22. Standard deviation for bulk samples is 0.15 for  $\delta^{13}\text{C}$  and 0.1 for  $\delta^{15}\text{N}$ .

## Results

We analysed 30 samples (Figs. 4 and 5) from the Velkerri Formation at a sampling resolution of 1 sample every ~11m.  $\delta^{15}\text{N}_{\text{bulk}}$  varies from +1.04‰ to +2.67‰ while  $\delta^{13}\text{C}_{\text{org}}$  varies from -35.2‰ to -32.4‰. Statistically significant correlations exist between  $\delta^{15}\text{N}_{\text{bulk}}$ ,  $\delta^{13}\text{C}_{\text{org}}$ , and TOC (at  $\alpha = 0.05$ ). Atomic C:N ratios range from 17.2 to 49.8.

**Alteration.** While it has been shown that changes in the nitrogen isotope characteristics of organic matter can occur during particle sinking and diagenesis (e.g. ref.<sup>42</sup>), it has also been shown that in high sediment accumulation zones, such as continental margins, no significant alteration of primary  $\delta^{15}\text{N}$  occurs<sup>43–45</sup>. Furthermore, unaltered bulk sedimentary  $\delta^{15}\text{N}$  generally reflects the  $\delta^{15}\text{N}$  of bioavailable nitrogen<sup>23</sup>. While such work provides confidence in the fidelity of  $\delta^{15}\text{N}$  of organic-rich sediments, we have investigated the possibility of alteration,

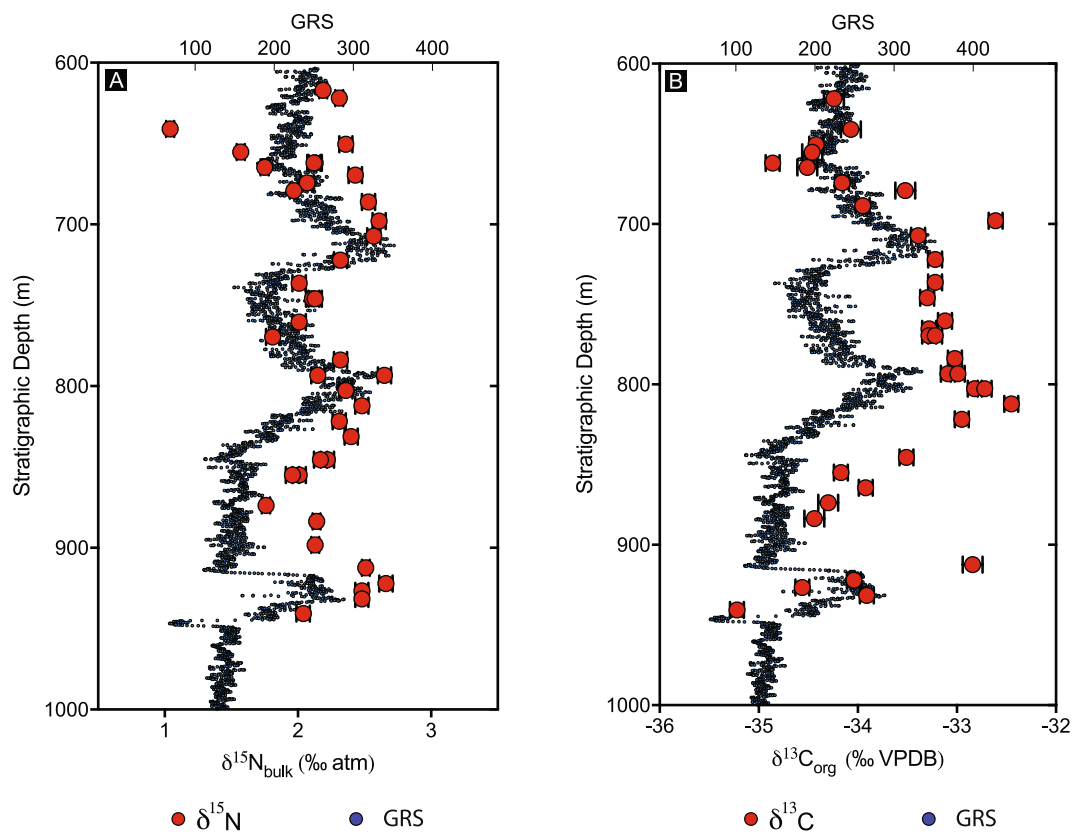


**Figure 5.** Up-section variations in  $\delta^{15}\text{N}_{\text{bulk}}$  (A) and  $\delta^{13}\text{C}_{\text{org}}$  (B) along with a gamma ray spectrum.

focussing on relationships between  $\delta^{15}\text{N}$  and thermal maturity, hydrocarbon generation, migration and devolatilisation (Fig. 6A–C), and find no evidence for the systematic alteration of  $\delta^{15}\text{N}$  via these processes. Furthermore, relationships between nitrogen abundance (N%), carbon abundance (C%) (Fig. 6D) and  $\text{K}_2\text{O}$  concentrations (%) (Fig. 6E) suggest that sources of inorganic nitrogen or exchangeable  $\text{NH}_4^+$  are negligible.

## Discussion

**Basin dynamics, primary productivity, redox, trace nutrients and the biogeochemical nitrogen cycle.** Measured nitrogen isotopes for the Velkerri Formation vary between +1.04‰ and +2.67‰, while measures of central tendency for this basinal facies have values that fall close to +2‰ (Fig. 7). Only a single sample has an isotopic value of  $\sim +1\%$ , a value that reasonably could be attributed solely to  $\text{N}_2$  fixation (i.e.  $-3\%$  to  $+1\%$ <sup>18</sup>), all other samples have  $\delta^{15}\text{N}$  values  $\geq +2\%$ , which are values consistent with aerobic nitrogen cycling<sup>16</sup>. Significantly, these variations in  $\delta^{15}\text{N}$  are not random but show statistically significant cycling at the 95% confidence level at a wavelength of  $\sim 110\text{m}$  (see Supplementary Information) and show consistent positive covariation with  $\delta^{13}\text{C}_{\text{org}}$ , TOC (Fig. 4) and GRS (Fig. 5). Considering that these cyclic changes in TOC and GRS are a regional feature of the basin, variations in  $\delta^{15}\text{N}$  and  $\delta^{13}\text{C}_{\text{org}}$  provide a basis for understanding the development of the observed cyclic organofacies.

**Lateral gradients in bioavailable nitrogen.** One possible explanation for the up-section variation we observe in  $\delta^{15}\text{N}$  could be that they represent lateral gradients in  $\delta^{15}\text{N}$  from near shore to offshore environments. Stüeken<sup>46</sup> argued for a lateral gradient in  $\delta^{15}\text{N}$  based on samples from the Mesoproterozoic Belt Supergroup. In this study,  $\delta^{15}\text{N}$  values varied from  $\sim -1\%$  in offshore basinal facies to  $\sim +5\%$  in near-shore facies. This trend was interpreted to reflect a transition from more productive coastal environments with active aerobic nitrogen cycling to nitrate poor offshore environments dominated by nitrogen fixation. A similar study for the Roper Group<sup>47</sup> identified a similar lateral gradient between platform ( $n = 4$ ) and basinal ( $n = 8$ ) facies, however, unlike the Belt Basin,  $\delta^{15}\text{N}$  values between basinal ( $n = 8$ ) and shelf ( $n = 22$ ) facies were statistically indistinguishable (Fig. 8).

Due to the near-shore–offshore lateral gradients observed in  $\delta^{15}\text{N}$  in some Mesoproterozoic basins<sup>46,47</sup>, it raises the possibility that the cycles observed in  $\delta^{15}\text{N}$  (Fig. 5A) represent subtle changes in water depth reflecting subtle changes in a lateral  $\delta^{15}\text{N}$  gradient. However, we think this is unlikely, as neither this study or previous studies<sup>30,41</sup> have shown any evidence for changes in water depth within the Amungee Member of the Velkerri Formation. Furthermore, the overall coarsening-upward sequence of the Velkerri Formation is well documented<sup>30,36,41</sup> and a prediction of this near shore–offshore gradient would be that both  $\delta^{15}\text{N}$  and  $\delta^{13}\text{C}$  should be isotopically heavier up-section (e.g. Fig. 8B & C), this is not observed (Fig. 5). However, our basinal facies are isotopically identical to basinal Velkerri samples from the wider basin and distinct from shallow water facies, this would indicate that the

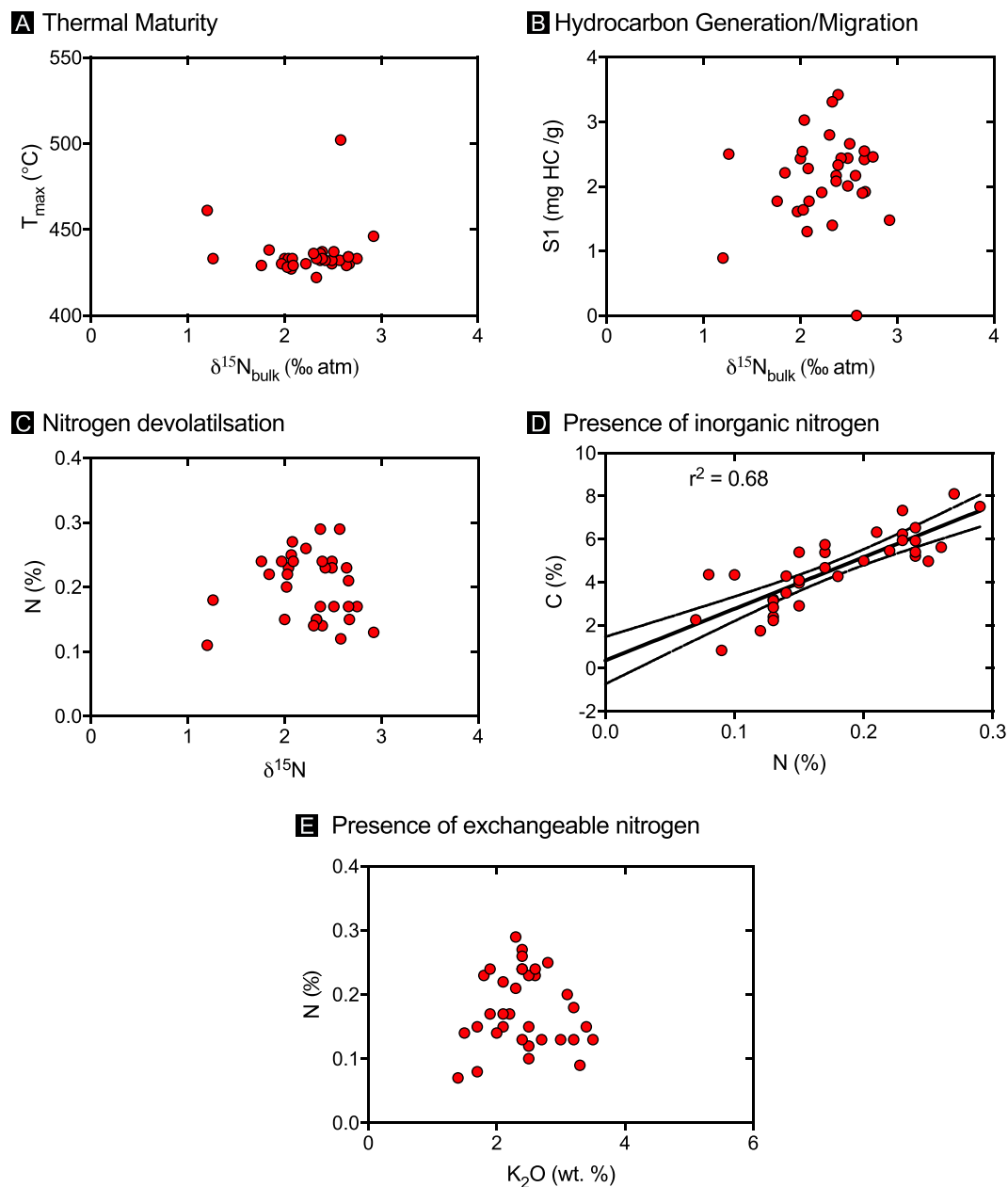


**Figure 6.** Possible secondary alteration of primary  $\delta^{15}\text{N}$  signatures due to (A) thermal maturity, (B) hydrocarbon generation and/or migration, (C) nitrogen devolatilisation, (D) presence of inorganic nitrogen and (E) exchangeable nitrogen.

organic enrichment of the Amungee Member of the Velkerri Formation is unlikely to be due to organic matter transported from shallower (i.e. shelf or platform, Fig. 8) near-shore environments, contrasting with previous suggestions<sup>33</sup>.

*Partial assimilation and/or partial nitrification.* If lateral variations do not provide a satisfactory explanation for the observed  $\delta^{15}\text{N}$  values, what mechanism can produce the observed range in  $\delta^{15}\text{N}$ , especially values greater than +2‰? Partial assimilation of bioavailable nitrogen could generate isotopically heavy  $\delta^{15}\text{N}$  as partial assimilation of  $\text{NH}_4^+$  leaves behind a residual pool of isotopically heavy nitrogen<sup>48</sup>. Furthermore, as assimilation of bioavailable nitrogen goes to completion in the modern nitrogen limited ocean<sup>42,49</sup>, it is unclear why partial assimilation would be a widespread characteristic considering the low levels of dissolved molybdenum estimated for the Mesoproterozoic<sup>50</sup>. Furthermore, modern analogues of Mesoproterozoic basins, such as the Black Sea and Cariaco Basins, also do not preserve evidence for partial assimilation<sup>49,51</sup>.

Partial nitrification of remineralised  $\text{NH}_4^+$  also has the ability to generate a  $^{15}\text{N}$  enriched residual pool<sup>52</sup>. However, considering that nitrification is rapid and occurs at vanishingly low levels of  $\text{O}_2$ <sup>53</sup>, it is expected to go to completion as nitrogen is widely considered the proximal limiting nutrient<sup>10,12</sup>.

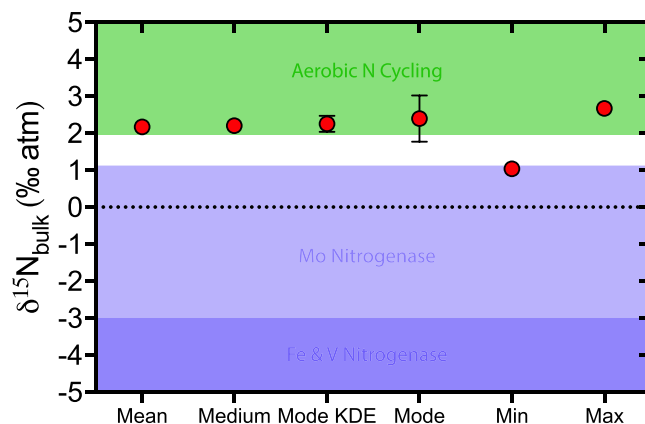


**Figure 7.** Measures of central tendency with 95% confidence intervals along with absolute minimum and maximum  $\delta^{15}\text{N}$  values. Field for Mo-Nitrogenase biomass is from ref.<sup>18</sup>.

**Denitrification.** A possible candidate to produce isotopically heavy  $\delta^{15}\text{N}$  would be partial denitrification either via heterotrophic denitrification and/or anaerobic ammonium oxidation. As denitrification occurs under low oxygen conditions, and water column redox is, in part, determined by the export and remineralisation of organic carbon from overlying surface waters, a dynamic feedback between organic matter production, export, remineralisation and denitrification can be envisaged. Furthermore, recent experimental results have shown that the rate of denitrification increases with increasing organic matter flux through the supply of fresh labile organic matter<sup>14</sup>. Such a dynamic feedback would provide a viable mechanism for producing cyclic enrichments in organic carbon, similar to those observed in the Velkerri Formation.

**Reduction in nitrogen fixation.** A further mechanism for generating isotopically heavy nitrogen was proposed by Anbar and Knoll<sup>11</sup>, who speculated that the redox sensitive behaviour of molybdenum, coupled with its role as a cofactor associated within MoFe-nitrogenase, the dominant and most efficient enzyme responsible for nitrogen fixation in diazotrophs<sup>54–56</sup>, may have implications bioavailable nitrogen (Mo-N co-limitation).

The basis for Mo-N co-limitation is that under oxic conditions molybdenum occurs as the soluble molybdate ion ( $\text{MoO}_4^{2-}$ ), however, under euxinic conditions, molybdenum reacts strongly with hydrogen sulphide to form the particle reactive thiomolybdate ion<sup>57</sup>. Thiomolybdates can be removed from seawater in organo-metallic complexes or within sulphide phases, resulting in molybdenum limitation. Recent work has shown that  $\text{N}_2$  fixation rates are reduced by ~80% at dissolved molybdenum concentrations between 1–5 nM<sup>58,59</sup>, such values are in the predicted range of dissolved molybdenum concentrations of Mesoproterozoic oceans<sup>50</sup>.

While it has been argued that euxinia and nitrate are mutually exclusive<sup>60</sup>, Stüeken *et al.*<sup>16</sup> pointed out that isotopically heavy  $\delta^{15}\text{N}$  has been documented in numerous Archean and Proterozoic basins inferred to have experienced euxinia, and suggested nitrate and euxinia are likely compatible in highly stratified waters. Euxinic conditions have been suggested in the Roper basin<sup>36,61</sup>. In particular, Cox *et al.*<sup>36</sup> noted enrichment in molybdenum in Velkerri sediments (up to ~100 ppm, twice the Mesoproterozoic average<sup>50</sup>) while biomarker studies<sup>62</sup> identified dibenzothiophene within the Amungee Member which at the very least suggests sulfate reduction within the sediments, however, together support transient deep-water euxinic conditions<sup>37,63–65</sup>.

Based on the boundaries for euxinia defined for the Velkerri Formation (~25 ppm Mo and ~4% TOC<sup>36</sup>), the comparison between molybdenum and  $\delta^{15}\text{N}$  reveals two distinct populations (Fig. 9). Samples with molybdenum concentrations below 25 ppm show variations in  $\delta^{15}\text{N}$  between ~+1‰ to ~+2.5‰. In contrast, samples containing more than 25 ppm molybdenum have  $\delta^{15}\text{N}$  exclusively above ~+2‰. Both a 2-tail *t*-test and Wilcoxon Signed Rank Test reveal that these two populations are statistically distinct ( $p = 0.0002$  at  $\alpha = 0.05$ ).

Typically, the shifting balance between nitrogen supply via  $\text{N}_2$  fixation (source of isotopically light  $\delta^{15}\text{N}$ ) and its loss via denitrification (producing isotopically heavy  $\delta^{15}\text{N}$  residual pool) is thought to be largely governed by basin redox conditions<sup>15,16,66</sup>. The dichotomy in the distribution of  $\delta^{15}\text{N}$  and molybdenum (Fig. 9) suggests that in those samples containing >25 ppm molybdenum, the balance between  $\text{N}_2$  fixation and denitrification was heavily biased towards denitrification. Considering the evidence for euxinia<sup>36,62</sup>, a parsimonious explanation would be molybdenum limitation affecting  $\text{N}_2$  fixation rates.

**Dynamic interplay between primary producers, basin redox and nitrogen cycling.** Partial assimilation and/or nitrification seem unlikely candidates controlling the variations observed in our  $\delta^{15}\text{N}$  record. Furthermore, while the range of  $\delta^{15}\text{N}$  values are completely consistent with values associated with offshore basinal facies (e.g. refs. 46,47), the cyclic variations cannot be explained by this mechanism, as it is incompatible with the detailed sedimentology of the Amungee Member and the overall high stand systems track for the Velkerri Formation.

The model proposed here envisages that during periods of high nutrient supply, as argued for the Amungee Member<sup>36</sup>, a cyclic process developed with high primary productivity and burial driving increasing levels of denitrification (i.e. ref.<sup>14</sup>). This process is suggested to have led to overall nitrogen limitation as denitrification ultimately depletes bioavailable nitrogen. However, the dichotomy in the distribution of  $\delta^{15}\text{N}$  and Mo (Fig. 9) and

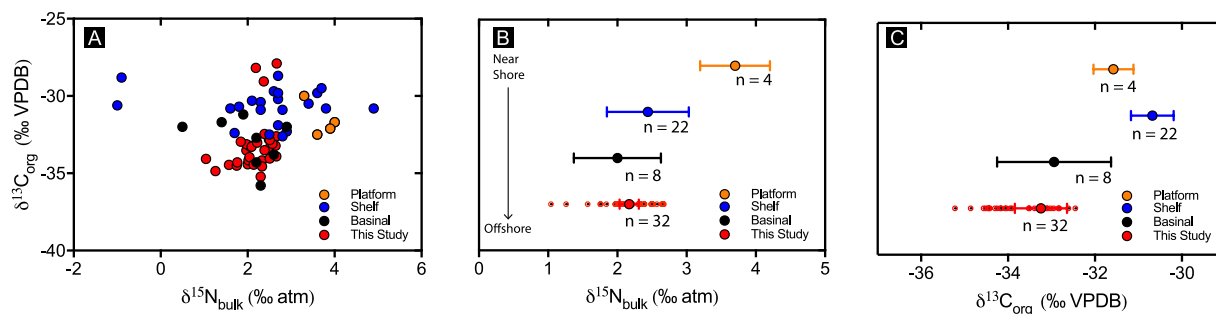


**Figure 8.** (A)  $\delta^{13}\text{C}$  vs.  $\delta^{15}\text{N}$ . (B,C) Average and 95% confidence intervals for platform (yellow), shelf (blue), and basinal (black) facies for the Roper Group (ref.<sup>47</sup>). Red data are from this study.

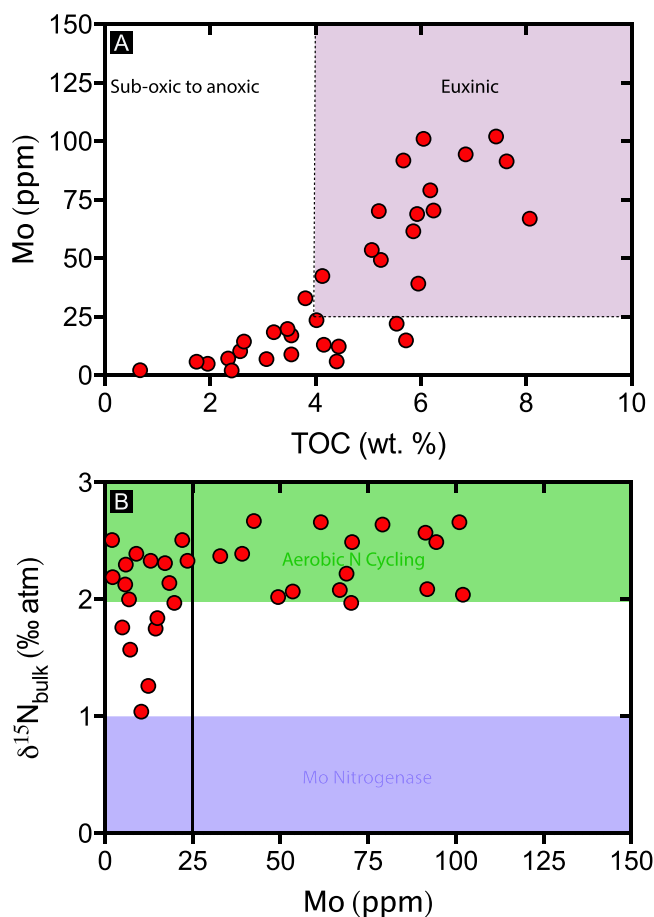


**Figure 9.** (A) Molybdenum vs. TOC and (B)  $\delta^{15}\text{N}$  vs. Mo. Euxinic conditions are interpreted to exist at molybdenum concentrations above 25 ppm and TOC above 4% from ref.<sup>36</sup>.

evidence for deep water euxinia suggests that a reduction in the concentration of dissolved molybdenum likely restricted  $\text{N}_2$  fixation as well through Mo-N co-limitation.

The consequence of increased denitrification and reduced  $\text{N}_2$  fixation is a reduction in primary productivity due to nitrogen limitation, a reduction in organic matter export/remineralisation and an easing of euxinic conditions. This ultimately resulted in increased levels of dissolved molybdenum, which shifted the balance towards renewed  $\text{N}_2$  fixation. Such a sequence of events is interpreted to have produced the cyclic variations between light and heavy  $\delta^{15}\text{N}$  along with positive covariations in TOC and  $\delta^{13}\text{C}$  seen in the Amunge Member.

While this discussion has centred around nitrogen, carbon isotopes also support this model. For the same reasons given for variations in  $\delta^{15}\text{N}$ ,  $\delta^{13}\text{C}$  variations do not reflect lateral environmental gradients in  $\delta^{13}\text{C}$ . They exhibit a positive correlation with TOC and as peaks in  $\delta^{15}\text{N}$  and TOC are associated with the most isotopically heavy  $\delta^{13}\text{C}$ , it is likely that these  $\delta^{13}\text{C}$  variations reflect changes in dissolved inorganic carbon, or more specifically, variations in contemporaneous organic carbon burial ( $f_{\text{org}}$ ), which likely reflect the strength of primary



productivity. These systematic positive covariations ( $\delta^{15}\text{N}$ ,  $\delta^{13}\text{C}$ , TOC, Mo) can be explained, ultimately, by changes in the balance between  $\text{N}_2$  fixation and denitrification resulting from the dynamic interaction between primary productivity, basin redox and biological metabolisms associated with nitrogen cycling. This biogeochemical model does not preclude higher order controls on the observed cyclicity such as orbital forcing mechanisms, however, available age constraints do not allow for a robust testing of such a higher order mechanism.

## Conclusions

Cyclic behaviour in organic matter enrichment within the Mesoproterozoic Velkerri Formation is not associated with maximum flooding surfaces or to variations in mineralogy or clastic flux. Nitrogen and carbon isotopes along with molybdenum concentrations record the shifting balance between  $\text{N}_2$  fixation and denitrification pathways which can be related to high levels of organic carbon production, export and variations in basin redox, specifically shifts between sub-oxic to euxinic conditions. The requirement of molybdenum in biological  $\text{N}_2$  fixation along with the efficient scavenging of molybdenum under euxinic conditions results in Mo-N co-limitation and a decrease in primary productivity. These feedbacks highlight the dynamic interplay between primary producers, basin redox and biogeochemical nitrogen cycling. Such interactions are important in constraining productivity in the marine biosphere and highlight that high levels of primary productivity and euxinia are inherently self-limiting. Furthermore, such feedbacks are important in understanding the development of Precambrian hydrocarbon source rocks, and more generally in understanding oxygenation of the ocean and atmosphere through Earth history; as all are ultimately related to organic carbon burial.

## Data Availability

All data that underlies this study can be found in Tables 1 through 3 in the accompanying supplementary information. Details of the well Altree-2 can be found at <http://www.geoscience.nt.gov.au/gemis/ngtgsjspu/handle/1/79405>.

## References

- Pedersen, T. F. & Calvert, S. E. Anoxia vs productivity; what controls the formation of organic-carbon-rich sediments and sedimentary rocks? *Am. Assoc. Pet. Geol. Bull.* **74**, 454–466 (1990).
- Condie, K. C., Des Marais, D. J. & Abbott, D. Precambrian superplumes and supercontinents: a record in black shales, carbon isotopes, and paleoclimates? *Precambrian Res.* **106**, 239–260 (2001).
- Meyer, K. M. & Kump, L. R. Oceanic Euxinia in Earth History: Causes and Consequences. *Annu. Rev. Earth. Planet. Sci.* **36**, 251–288 (2008).
- Hartnett, H. E., Keil, R. G., Hedges, J. I. & Devol, A. H. Influence of oxygen exposure time on organic carbon preservation in continental margin sediments. *Nature* **391**, 572–575 (1998).
- Kennedy, M. J., Pevear, D. R. & Hill, R. J. Mineral Surface Control of Organic Carbon in Black Shale. *Science* **295**, 657–660 (2002).
- Mayer, L. M. Surface area control of organic carbon accumulation in continental shelf sediments. *Geochim. Cosmochim. Acta.* **58**, 1271–1284 (1994).
- Hedges, J. I. & Keil, R. G. Sedimentary organic matter preservation: an assessment and speculative synthesis. *Marine Chemistry* **49**, 81–115 (1995).
- Müller, P. J. & Suess, E. Productivity, sedimentation rate, and sedimentary organic matter in the oceans—I. Organic carbon preservation. *Deep Sea Research Part A Oceanographic Research Papers* **26**, 1347–1362 (1979).
- Falkowski, P. G. Evolution of the nitrogen cycle and its influence on the biological sequestration of  $\text{CO}_2$  in the ocean. *Nature* **387**, 272–275 (1997).
- Tyrrell, T. The relative influences of nitrogen and phosphorus on oceanic primary production. *Nature* **400**, 525–531 (1999).
- Anbar, A. D. & Knoll, A. H. Proterozoic ocean chemistry and evolution: a bioinorganic bridge? *Science* **297**, 1137–1142 (2002).
- Bristow, L. A., Mohr, W., Ahmerkamp, S. & Kuypers, M. M. M. Nutrients that limit growth in the ocean. *Current Biology* **27**, R474–R478 (2017).
- Johnston, D. T. *et al.* An emerging picture of Neoproterozoic ocean chemistry: Insights from the Chuar Group, Grand Canyon, USA. *Earth Planet. Sci. Lett.* **290**, 64–73 (2010).
- Babbín, A. R., Keil, R. G., Devol, A. H. & Ward, B. B. Organic Matter Stoichiometry, Flux, and Oxygen Control Nitrogen Loss in the Ocean. *Science* **344**, 406 (2014).
- Ader, M. *et al.* Interpretation of the nitrogen isotopic composition of Precambrian sedimentary rocks: Assumptions and perspectives. *Chemical Geology* **429**, 93–110 (2016).
- Stüeken, E. E., Kipp, M. A., Koehler, M. C. & Buick, R. The evolution of Earth's biogeochemical nitrogen cycle. *Earth-Science Reviews* **160**, 220–239 (2016).
- Planavsky, N. J. *et al.* Widespread iron-rich conditions in the mid-Proterozoic ocean. *Nature* **477**, 448–451 (2011).
- Bauersachs, T. *et al.* Nitrogen isotopic fractionation associated with growth on dinitrogen gas and nitrate by cyanobacteria. *Limnology and Oceanography* **54**, 1403–1411 (2009).
- Wade, E. Nitrogen Isotope Fractionation and Its Significance in Biogeochemical Processes Occurring in Marine Environments. In: Goldberg ED, Horibe T, Saruhashi K (eds). *Isotope Marine Chemistry*: Uchida Rokakuho (1980).
- Brunner, B. *et al.* Nitrogen isotope effects induced by anammox bacteria. *Proc. Natl. Acad. Sci. USA* **110**, 18994 (2013).
- Hoch, M. P., Fogel, M. L. & Kirchman, D. L. Isotope fractionation associated with ammonium uptake by a marine bacterium. *Limnology and Oceanography* **37**, 1447–1459 (1992).
- McCready, R. G. L., Gould, W. D. & Barendregt, R. W. Nitrogen isotope fractionation during the reduction of  $\text{NO}_3^-$  to  $\text{NH}_4^+$  by *Desulfovibrio* sp. *Canadian Journal of Microbiology* **29**, 231–234 (1993).
- Galbraith E. D., Sigman D. M., Robinson R. S. & Pedersen T. F. Chapter 34 - Nitrogen in Past Marine Environments. *Nitrogen in the Marine Environment (2nd Edition)*. Academic Press: San Diego, 1497–1535 (2008).
- Lam, P. *et al.* Revising the nitrogen cycle in the Peruvian oxygen minimum zone. *Proc. Natl. Acad. Sci. USA* **106**, 4752 (2009).
- Prokopenko, M. G. *et al.* Nitrogen cycling in the sediments of Santa Barbara basin and Eastern Subtropical North Pacific: Nitrogen isotopes, diagenesis and possible chemosymbiosis between two lithotrophs (*Thioploca* and *Anammox*)—"riding on a glider". *Earth Planet. Sci. Lett.* **242**, 186–204 (2006).
- Sigman, D. M. *et al.* The dual isotopes of deep nitrate as a constraint on the cycle and budget of oceanic fixed nitrogen. *Deep Sea Research Part I: Oceanographic Research Papers* **56**, 1419–1439 (2009).
- Rawlings, D. J. Stratigraphic resolution of a multiphase intracratonic basin system: the McArthur Basin, northern Australia. *Aust. Jour. of Earth. Sci.* **46**, 703–723 (1999).

28. Jackson, M. J., Muir, M. D. & Plumb, K. A. Geology of the southern McArthur Basin, Northern Territory. Bureau of Mineral Resources, Geology and Geophysics (1987).
29. Lindsay, J. F. Basin dynamics and mineralisation, McArthur Basin, northern Australia. *Aust. Jour. of Earth. Sci.* **48**, 703–720 (2001).
30. Abbott, S. T. & Sweet, I. P. Tectonic control on third-order sequences in a siliciclastic ramp-style basin: An example from the Roper Superbasin (Mesoproterozoic), northern Australia. *Aust. Jour. of Earth. Sci.* **47**, 637–657 (2000).
31. Rawlings D. J. *et al.* The 2002 Southern McArthur Basin Seismic Reflection Survey. Geoscience Australia (2004).
32. Plumb, K. A. & Wellman, P. McArthur Basin, Northern Territory: mapping of deep troughs using gravity and magnetic anomalies. *BMR Journal of Australian Geology and Geophysics.* **10**, 243–251 (1997).
33. Sheridan, M., Johns, R. D., Johnson, H. D. & Menpes, S. The stratigraphic architecture, distribution and hydrocarbon potential of the organic-rich Kyalla and Velkerri shales of the Upper Roper Group (McArthur Basin). *The APPEA Journal.* **58**, 858–864 (2018).
34. Kendall, B., Creaser, R. A., Gordon, G. W. & Anbar, A. D. Re–Os and Mo isotope systematics of black shales from the Middle Proterozoic Velkerri and Wollgorang Formations, McArthur Basin, northern Australia. *Geochim. Cosmochim. Acta.* **73**, 2534–2558 (2009).
35. Yang, B. *et al.* Spatial and temporal variation in detrital zircon age provenance of the hydrocarbon-bearing upper Roper Group, Beetaloo Sub-basin, Northern Territory, Australia. *Precambrian Res.* **304**, 140–155 (2018).
36. Cox, G. M. *et al.* Basin redox and primary productivity within the Mesoproterozoic Roper Seaway. *Chemical Geology.* **440**, 101–114 (2016).
37. Revie, D. *Unconventional petroleum resources of the Roper Group, McArthur Basin.* Northern Territory Geological Survey: Darwin (2016).
38. Jackson, M. J., Powell, T. G., Summons, R. E. & Sweet, I. P. Hydrocarbon shows and petroleum source rocks in sediments as old as  $1.7 \times 10^9$  years. *Nature* **322**, 727–729 (1986).
39. Close, D. I. *et al.* Proterozoic shales gas plays in the Beetaloo Basin and the Amungee NW-1H discovery. *AGES 2017.* Alice Springs: Northern Territory Geological Survey. 91–97 (2017).
40. Munson, T. J. & Revie, D. Stratigraphic subdivision of Velkerri Formation, Roper Group, McArthur Basin, Northern Territory. *Northern Territory Geological Survey Record* 2018–006 (2018).
41. Warren, J. K., George, S. C., Hamilton, P. J. & Tingate, P. Proterozoic Source Rocks: Sedimentology and Organic Characteristics of the Velkerri Formation, Northern Territory, Australia. *Am. Assoc. Pet. Geol. Bull.* **82**, 442–443 (1998).
42. Altabet, M. A. & Francois, R. Sedimentary nitrogen isotopic ratio as a recorder for surface ocean nitrate utilization. *Global Biogeochemical Cycles* **8**, 103–116 (1994).
43. Altabet, M. A. Nitrogen and Carbon Isotopic Tracers of the Source and Transformation of Particles in the Deep Sea. In: Ittekkot V (ed). *Particle Flux in the Ocean.* John Wiley: New York, pp 155–171 (1996).
44. Kienast, S. S., Calvert, S. E. & Pedersen, T. F. Nitrogen isotope and productivity variations along the northeast Pacific margin over the last 120 kyr: Surface and subsurface paleoceanography. *Paleoceanography.* **17**, 1–17 (2002).
45. Thunell, R. C., Sigman, D. M., Muller-Karger, F., Astor, Y. & Varela, R. Nitrogen isotope dynamics of the Cariaco Basin, Venezuela. *Global Biogeochemical Cycles* **18**, 1–13 (2004).
46. Stüeken, E. E. A test of the nitrogen-limitation hypothesis for retarded eukaryote radiation: Nitrogen isotopes across a Mesoproterozoic basinal profile. *Geochim. Cosmochim. Acta.* **120**, 121–139 (2013).
47. Koehler, M. C., Stüeken, E. E., Kipp, M. A., Buick, R. & Knoll, A. H. Spatial and temporal trends in Precambrian nitrogen cycling: A Mesoproterozoic offshore nitrate minimum. *Geochim. Cosmochim. Acta.* **198**, 315–337 (2017).
48. Casciotti, K. L. Inverse kinetic isotope fractionation during bacterial nitrite oxidation. *Geochim. Cosmochim. Acta.* **73**, 2061–2076 (2009).
49. Fulton, J. M., Arthur, M. A. & Freeman, K. H. Black Sea nitrogen cycling and the preservation of phytoplankton  $\delta^{15}\text{N}$  signals during the Holocene. *Global Biogeochemical Cycles.* **26** (2012).
50. Reinhard, C. T. *et al.* Proterozoic ocean redox and biogeochemical stasis. *Proc. Natl. Acad. Sci. USA* **110**, 5357–5362 (2013).
51. Haug, G. H. *et al.* Glacial/interglacial variations in production and nitrogen fixation in the Cariaco Basin during the last 580 kyr. *Paleoceanography.* **13**, 427–432 (2010).
52. Casciotti, K. L., Sigman, D. M. & Ward, B. B. Linking Diversity and Stable Isotope Fractionation in Ammonia-Oxidizing Bacteria. *Geomicrobiology Journal.* **20**, 335–353 (2003).
53. Fuchsman, C. A., Murray, J. W. & Kononov, S. K. Concentration and natural stable isotope profiles of nitrogen species in the Black Sea. *Marine Chemistry.* **111**, 90–105 (2008).
54. Burgess, B. K. & Lowe, D. J. Mechanism of Molybdenum Nitrogenase. *Chemical Reviews.* **96**, 2983–3012 (1996).
55. Hoffman, B. M., Lukoyanov, D., Yang, Z.-Y., Dean, D. R. & Seefeldt, L. C. Mechanism of Nitrogen Fixation by Nitrogenase: The Next Stage. *Chemical Reviews.* **114**, 4041–4062 (2014).
56. Joerger, R. D., Bishop, P. E. & Evans, H. J. Bacterial Alternative Nitrogen Fixation Systems. *Critical Reviews in Microbiology.* **16**, 1–14 (1988).
57. Scott, C. & Lyons, T. W. Contrasting molybdenum cycling and isotopic properties in euxinic versus non-euxinic sediments and sedimentary rocks: Refining the paleoproxies. *Chemical Geology.* **324–325**, 19–27 (2012).
58. Zerkle, A. L., House, C. H., Cox, R. P. & Canfield, D. E. Metal limitation of cyanobacterial  $\text{N}_2$  fixation and implications for the Precambrian nitrogen cycle. *Geobiology.* **4**, 285–297 (2006).
59. Glass, J., Axler, R., Chandra, S. & Goldman, C. Molybdenum limitation of microbial nitrogen assimilation in aquatic ecosystems and pure cultures. *Frontiers in Microbiology.* **3**, 331 (2012).
60. Boyle, R. A. *et al.* Nitrogen cycle feedbacks as a control on euxinia in the mid-Proterozoic ocean. *Nature Comms.* **4**, 1533 (2013).
61. Shen, Y., Canfield, D. E. & Knoll, A. H. Middle Proterozoic ocean chemistry: Evidence from the McArthur Basin, northern Australia. *Amer. Jour. of Sci.* **302**, 81–109 (2002).
62. Jarrett, A. J. *et al.* Microbial assemblage and palaeoenvironmental reconstruction of the 1.38 Ga Velkerri Formation, McArthur Basin, northern Australia. *Geobiology.* **00**, 1–21 (2019).
63. Lyons, T. W., Anbar, A. D., Severmann, S., Scott, C. & Gill, B. C. Tracking Euxinia in the Ancient Ocean: A Multiproxy Perspective and Proterozoic Case Study. *Annual Review of Earth and Planetary Sciences.* **37**, 507–534 (2009).
64. Tribouillard, N., Algeo, T. J., Lyons, T. & Riboulleau, A. Trace metals as paleoredox and paleoproductivity proxies: An update. *Chemical Geology.* **232**, 12–32 (2006).
65. Mizukami, T., Kaiho, K. & Oba, M. Significant changes in land vegetation and oceanic redox across the Cretaceous/Paleogene boundary. *Palaeogeography, Palaeoclimatology, Palaeoecology.* **369**, 41–47 (2013).
66. Zerkle, A. L. & Mikhail, S. The geobiological nitrogen cycle: From microbes to the mantle. *Geobiology.* **15**, 343–352 (2017).

## Acknowledgements

GMC and MLB are supported by an Australian Research Council Linkage grant (LP16010135). Linkage grant partners include Santos, Origin Energy, Imperial Oil and Gas, University of Adelaide, Wollongong University, the Czech Academy of Sciences and the Northern Territory Geological Survey. All partners are thanked for access to core and other resources.

### Author Contributions

G.M.C. conceived the project and interpreted the data. All authors contributed in the writing of the manuscript and supplementary material.

### Additional Information

**Supplementary information** accompanies this paper at <https://doi.org/10.1038/s41598-019-40783-4>.

**Competing Interests:** The authors declare no competing interests.

**Publisher's note:** Springer Nature remains neutral with regard to jurisdictional claims in published maps and institutional affiliations.



**Open Access** This article is licensed under a Creative Commons Attribution 4.0 International License, which permits use, sharing, adaptation, distribution and reproduction in any medium or format, as long as you give appropriate credit to the original author(s) and the source, provide a link to the Creative Commons license, and indicate if changes were made. The images or other third party material in this article are included in the article's Creative Commons license, unless indicated otherwise in a credit line to the material. If material is not included in the article's Creative Commons license and your intended use is not permitted by statutory regulation or exceeds the permitted use, you will need to obtain permission directly from the copyright holder. To view a copy of this license, visit <http://creativecommons.org/licenses/by/4.0/>.

© The Author(s) 2019